Available online www.jocpr.com

Journal of Chemical and Pharmaceutical Research

J. Chem. Pharm. Res., 2011, 3(5):323-339

ISSN No: 0975-7384
CODEN(USA): JCPRC5

Molecular structure, spectroscopic (FT-IR, FT-Raman, NMR) studies and first-order molecular hyperpolarizabilities of 5-amino-2-hydroxybenzoic acid (5A2HBA) by *ab initio* HF and density functional method

S. Muthu[a] and E. Isac Paulraj[b*]

[a]*Department of Physics, Sri Venkateswara College of Engineering, Sriperumbudur, India*
[b]*Department of Physics, Pallavan College of Engineering, Kancheepuram, India*

ABSTRACT

The Fourier transform infrared (FT-IR) and FT Raman spectra of 5-amino-2-hydroxybenzoic acid (5A2HBA) have been recorded in the regions 4000–400 and 4000–100 cm^{-1}, respectively. 5-amino-2-hydroxybenzoic acid is used as an anti-inflammatory agent .The optimized geometry, frequency and intensity of the vibrational bands of (5A2HBA) were obtained by ab initio and DFT levels of theory with complete relaxation in the potential energy surface using 6-31G(d,p) basis set. A complete vibrational assignment aided by the theoretical harmonic frequency analysis has been proposed. The harmonic vibrational frequencies, infrared intensities and Raman scattering activities, force constants are calculated by ab initio HF and DFT B3LYP methods with 6-31G(d,p) basis set. Stability of the molecule arising from hyper conjugative interactions, charge delocalization has been analyzed using natural bond orbital (NBO) analysis. The results show that charge in electron density (ED) in the σ and π* anti bonding orbitals and E2 energies confirms the occurrence of ICT (Intra molecular Charge Transfer) within the molecule. ^{13}C and ^{1}H NMR chemical shifts results were given and are in agreement with the corresponding experimental values. Highest occupied molecular orbital (HOMO) - lowest unoccupied molecular orbital (LUMO) energy gaps were studied. The scaled theoretical wavenumbers show good agreement with the experimental values. Comparison of the simulated spectra with the experimental spectra provides important information about the ability of the computational method to describe the vibrational modes.*

Keywords: FTIR and FT Raman spectra; Ab initio HF and DFT; Vibrational analysis; ^{13}C and ^{1}H NMR chemical shifts; NBO analysis; 5-amino-2-hydroxybenzoic acid (5A2HBA).

INTRODUCTION

5-amino-2-hydroxybenzoic acid (5A2HBA) belongs to the class of aminosalicylates. It has a bright orange-yellow colour with molecular formula $C_7H_7NO_3$.. It is chemically called as 5-amino-2-hydroxybenzoic acid. 5A2HBA is the active component of sulfasalazine. It is soluble in water and slightly soluble in alcohol but it is insoluble in ethanol. Pharmaceutically it is an anti-inflammatory drug used to treat inflammation of the digestive tract (Crohn's disease) and mild to moderate ulcerative colitis. It is used in the synthesis of other organic compounds including pharmaceuticals. Synthesis and other investigations on the title compound and its derivatives have been carried out by many researchers. The role of a novel H_2S-releasing derivative of mesalamine (5-amino-2-hydroxybenzoic acid) were reported[1].

Synthesis and antimicrobial activities of 5-amino-2-hydroxybenzoic acid were reported [2]. Enhanced activity of a hydrogen sulphide-releasing derivative of mesalamine in a mouse model of colitis were reported [3]. Green approach for large scale process of mesalamine were reported [4]. Literature survey reveals that to the best of our knowledge no ab initio HF/DFT frequency calculations of 5A2HBA have been reported so far. As a result we set out experimental and theoretical investigation of the vibrational and NMR spectra of this molecule. Quantum chemical computational methods have proved to be an essential tool for interpreting and predicting the vibrational spectra[5,6]. Now-a-days, sophisticated electron correlation and density functional theory calculations are increasingly available and deliver force fields of high accuracy even for large polyatomic molecules[7]. Hence in this study, an attempt has been made to interpret the vibrational spectra of 5A2HBA by applying Hartree Fock theory and density functional theory calculations based on Becke3–Lee–Yang–Parr (B3LYP) and 6-31G(d,p) basis set. Ab initio HF and density functional theory (DFT) calculations have been performed to support our wavenumber assignments.

EXPERIMENTAL DETAILS

The compound 5A2HBA was purchased from Sigma–Aldrich chemical company, USA with more than 98% purity and was used as such without further purification to record FTIR and FT Raman spectra. The FTIR spectrum of the compound was recorded in the region 4000–400 cm^{-1} in evacuation mode on Bruker IFS 66V spectrophotometer using KBr pellet technique (solid phase). The spectrum was recorded at room temperature, with a spectral resolution of 2.0 cm^{-1} and the number of co-added scans was 50 for each spectrum.

The FT-Raman spectrum of 5A2HBA was also recorded in the region 4000–100 cm^{-1} with the same instrument equipped with FRA 106 Raman module accessory. A Nd: YAG laser source operating at 1.064 μm line widths with 200 mW power was used for excitation. The frequencies of all sharp bands are accurate to ±1 cm^{-1}. The labelling of atoms in 5A2HBA is given in Fig. 1. The experimental FT-IR and FT-Raman spectra along with theoretically predicted infrared and Raman spectra are shown in Figs 2 and 3 respectively. The ^1H and ^{13}C NMR spectra were recorded on a Bruker AMX 400 MHz for ^1H and 100 MHz for ^{13}C NMR in DMSO-d6 with TMS as an internal standard, at Indian Institute of Science, Bangalore, India. ^1H and ^{13}C NMR spectra are shown in Figs. 4 and 5 respectively.

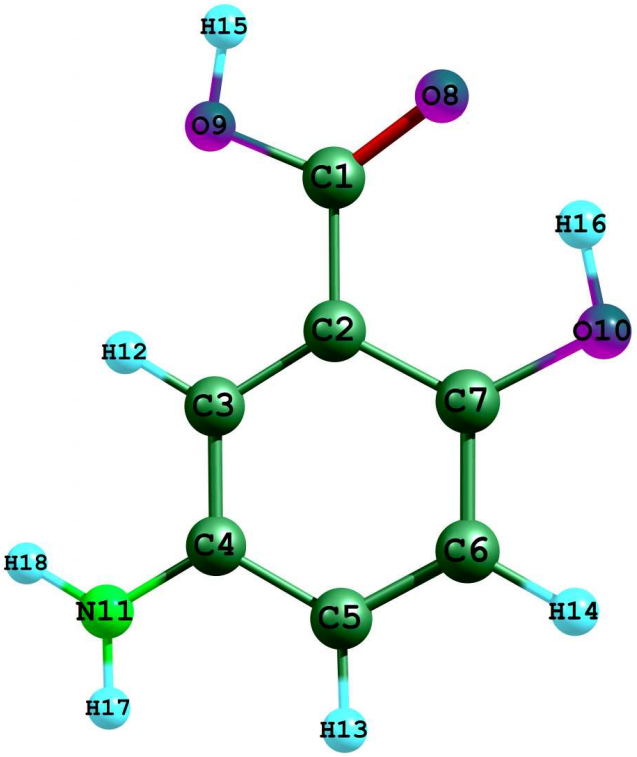

Fig. 1 The atom numbering for 5A2HBA molecule

Computational Details

The entire calculations were performed at Hartree-Fock (HF) and B3LYP levels on a Intel core2Duo 1.8 GHz personal computer using Gaussian 03W program package [8], invoking gradient geometry optimization [9]. Initial geometry generated from standard geometrical

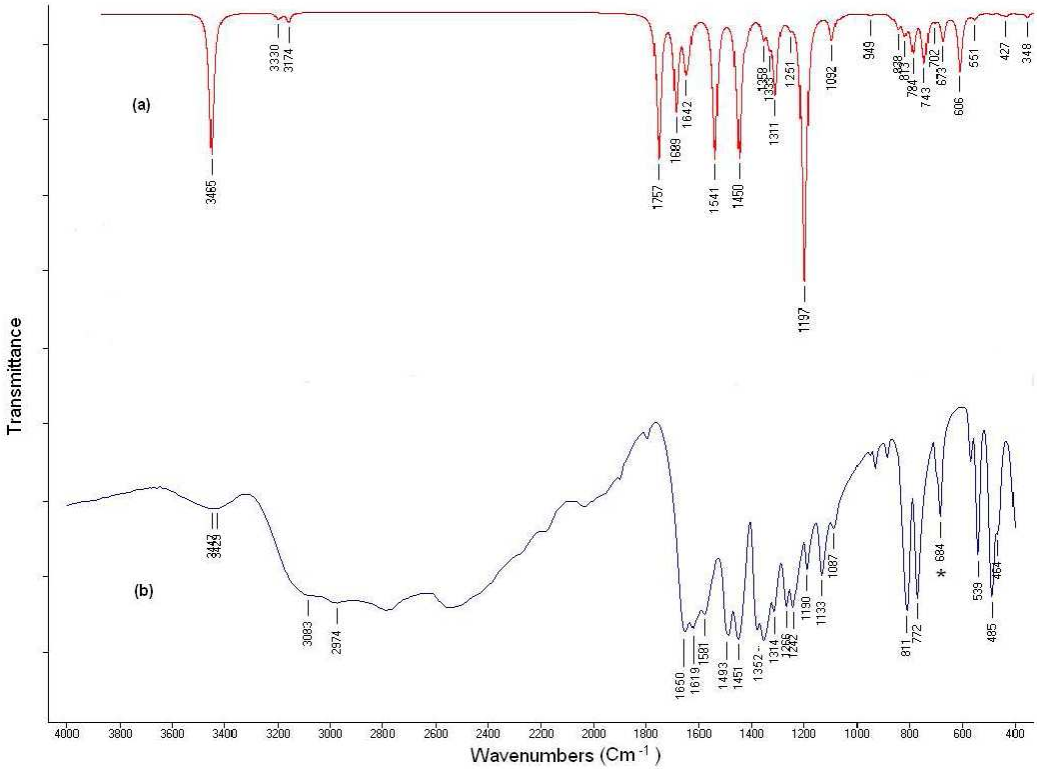

Fig. 2 FTIR spectra of 5A2HBA, (a) calculated and (b) observed

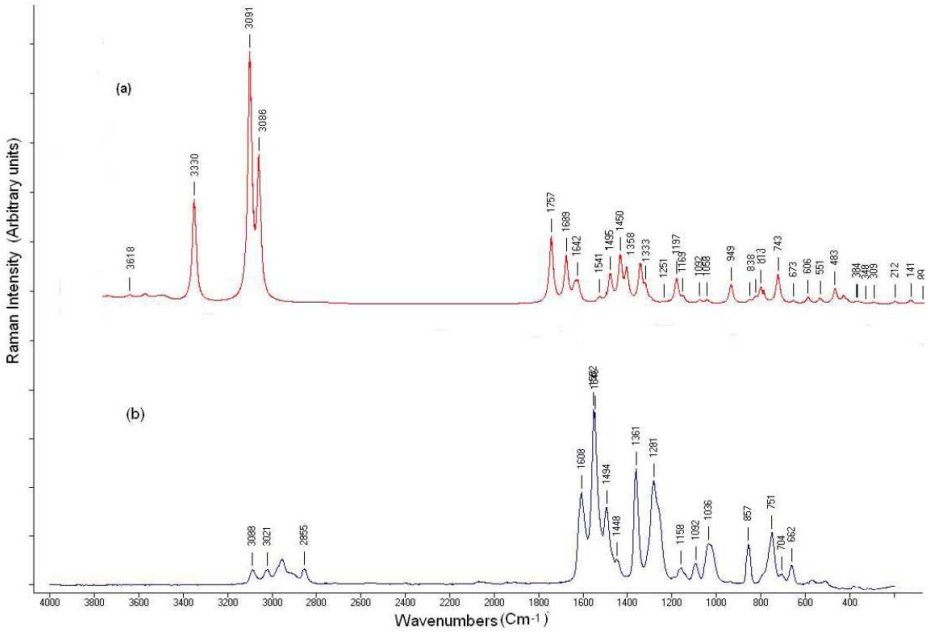

Fig. 3 FT Raman spectra of 5A2HBA, (a) calculated and (b) observed

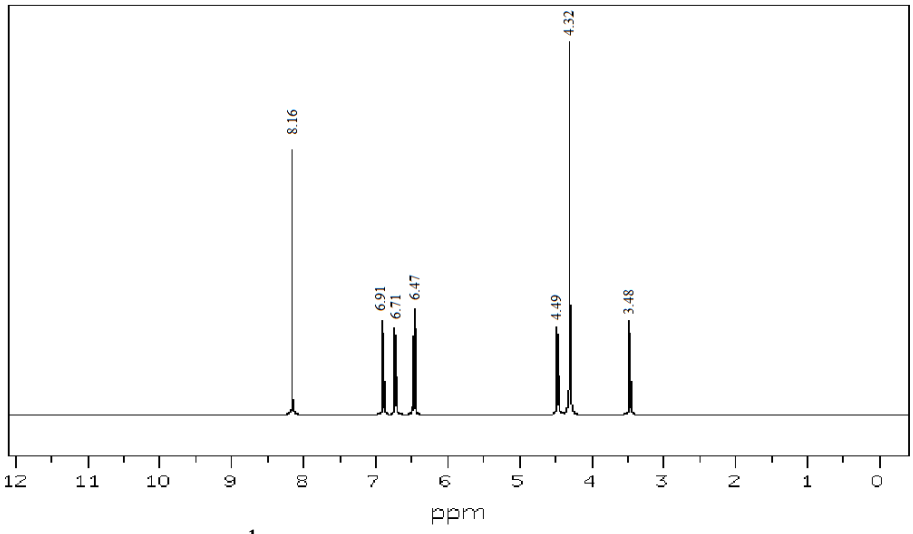

Fig. 4 ^{1}H NMR spectra of 5A2HBA in DMSO-d6

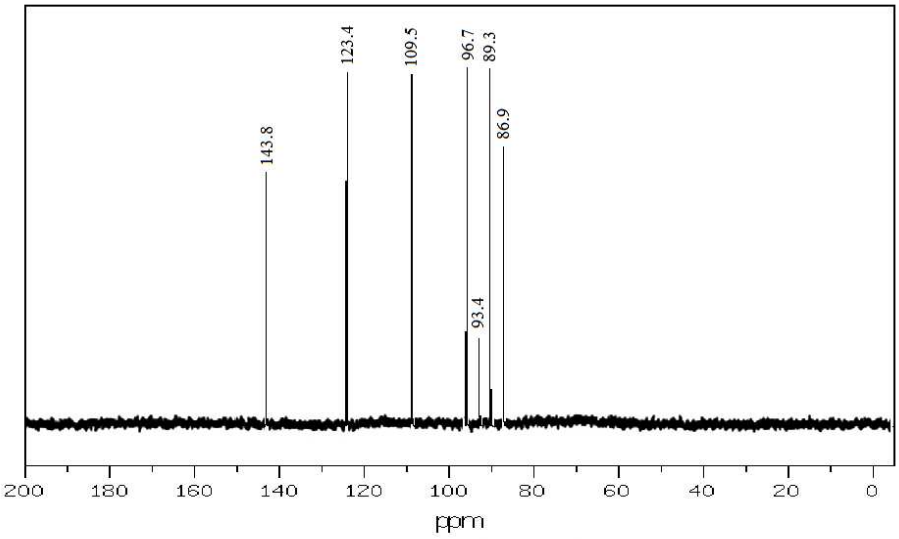

Fig. 5 ^{13}C NMR spectra of 5A2HBA in DMSO-d6

parameters was minimized without any constraint in the potential energy surface at Hartree-Fock level, adopting the standard 6-31G(d,p) basis set. This geometry was then re-optimized again at B3LYP level [10] using the same basis set 6-31G(d.p) for better description. The optimized structural parameters were used in the vibrational frequency calculation to characterize all stationary points as minima. Using Chemcraft program [11] with symmetry considerations along with available related molecules, vibrational frequency assignments were made with a high degree of accuracy. The wavenumber values computed at the HF and DFT levels contains known systematic errors due to the negligence of electron correlation [12]. Therefore, we have used a scaling factor value of 0.902 for the HF/6-31G(d,p) basis set and 0.960 for the B3LYP/6-31G(d,p) basis set [13]. It should be noted that Gaussian 03 package does not calculate the Raman intensity. The Raman activities were transformed into Raman intensities using RaInt program [14] by the expression:

$$I_i = 10^{-12} (\nu_0 - \nu_i)^4 (1/\nu_i) S_i$$

Where I_i is the Raman intensity, S_i is the Raman scattering activities, ν_i is the wavenumber of normal modes, and ν_o denotes the wavenumber of the excitation laser [15]. Next, the spectra were analyzed in terms of the P.E.D. contributions by using the VEDA program [16].

RESULTS AND DISCUSSION

Molecular geometry

The optimized structure parameters of 5A2HBA calculated by ab initio HF and DFT-B3LYP levels with the 6-31G(d,p) basis set are listed in the Table 1 in accordance with the atom numbering scheme given in Fig.1. Table 1 compares the calculated bond lengths and angles for 5A2HBA with those experimentally available from x-ray diffraction data [17].

The experimental and calculated geometric parameters agree well with almost all values. The small deviations are probably due to the theoretical calculations belong to isolated molecules in gaseous phase and the experimental results belong to molecules in solid state. The frequency values computed at B3LYP level contains known systematic error. Therefore, linearity between the experimental and calculated vibrational frequency can be estimated by plotting the calculated values against experimental frequency (shown in Fig.6). Certain values obtained between the two methods, are strongly underestimated. If the variations are omitted, B3LYP calculations provide good linearity between the calculated and experimental frequencies.

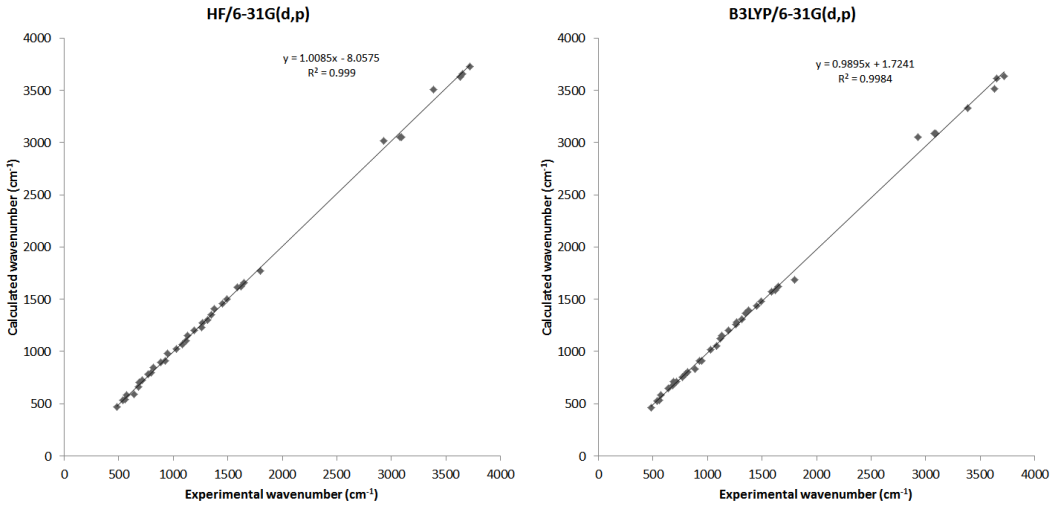

Fig. 6. Comparative graph of experimental frequency and computed frequency (HF and DFT)

Table 1 Optimized geometrical parameters of *Mesalazine* molecules, bond length (A°), interaxial angles (◦)

Parameters	Expt	HF/6-31G(d,p)	B3LYP/ 6-31G(d,p)
		Bond Length	
C_1-C_2	1.52	1.47	1.46
C_1-O_8	1.21	1.20	1.23
C_1-O_9	1.34	1.32	1.35
C_2-C_3	1.42	1.40	1.41
C_2-C_7	1.42	1.39	1.42
C_3-C_4	1.42	1.38	1.39
C_3-H_{12}	1.10	1.07	1.09
C_4-C_5	1.42	1.40	1.41
C_4-N_{11}	1.46	1.38	1.38
C_5-C_6	1.42	1.37	1.38
C_5-H_{13}	1.10	1.08	1.09
C_6-C_7	1.42	1.40	1.40
C_6-H_{14}	1.10	1.07	1.09
C_7-O_{10}	1.36	1.34	1.35
O_9-H_{15}	0.97	0.95	0.97
O_{10}-H_{16}	0.97	0.95	0.98
N_{11}-H_{17}	1.05	0.99	1.00
N_{11}-H_{18}	1.05	0.99	1.00
Bond Angle			
C_2-C_1-O_8	123.0	124.6	124.7
C_2-C_1-O_9	124.3	114.7	115.1
C_1-C_2-C_3	117.6	120.4	121.3
C_1-C_2-C_7	117.6	119.4	118.4
O_8-C_1-O_9	122.0	120.7	120.3
C_1-O_9-H_{15}	106.1	107.9	105.7
C_3-C_2-C_7	120.0	120.2	120.3
C_2-C_3-C_4	120.0	121.4	121.2
C_2-C_3-H_{12}	120.0	118.6	118.6
C_2-C_7-C_6	120.0	118.2	118.2
C_2-C_7-O_{10}	124.3	124.6	123.5
C_4-C_3-H_{12}	120.0	119.9	120.2
C_3-C_4-C_5	120.0	117.6	117.8
C_3-C_4-N_{11}	120.0	121.9	121.7
C_5-C_4-N_{11}	120.0	120.5	120.5
C_4-C5-C6	120.0	121.5	121.6
C_4-C_5-H_{13}	120.0	119.3	119.2
C_4-N_{11}-H_{17}	120.0	121.0	121.0
C_4-N_{11}-H_{18}	120.0	120.9	121.0
C_6-C_5-N_{13}	120.0	119.1	119.2
C_5-C_6-C_7	120.0	121.0	120.9
C_5-C_6-H_{14}	120.0	120.9	120.9
C_7-C_6-H_{14}	120.0	118.2	118.2
C_6-C_7-O_{10}	124.3	117.1	118.3
C_7-O_{10}-H_{16}	108.0	110.0	106.9
H_{17}-N_{11}-H_{18}	118.8	118.1	118.0

Vibrational band assignment

Infrared and Raman spectra contain a number of bands at specific wavenumbers. The aim of the vibrational analysis is to decide which of the vibrational modes give rise to each of these observed bands. The assignments for the fundamental modes of vibrations have been made on the basis of the position shape and intensity. Vibrational frequencies of derivatives of benzene [18,19] have been taken into consideration for the assignment of fundamental vibrations of 5A2HBA. The observed FT-IR and FT-Raman frequencies for various modes of vibrations are presented in Table 2. The last column of Table 2 shows the detailed vibrational assignment obtained from the calculated potential energy distribution (PED). Comparison of the frequencies calculated at HF and B3LYP with the experimental values (Table 2), reveals the overestimation of calculated vibrational modes due to neglect of anharmonicity in real system. Inclusion of electron correlation in density functional theory to a certain extend makes the frequency values smaller in comparison with the HF frequency data.

Table – 2 Vibrational wave numbers obtained for mesalazine at HF/6-31G(d,p) and B3LYP/6-31G(d,p) [harmonic wave number (cm-1) IR intensities (km mol-1), Raman scattering activities (A0 amu-1), and force constants (m dyn A0-1)

Mode no.	Experimental Wave number		Calculated Wave number		HF/6-31G(d,p)		B3LYP/6-31G(d,p)		HF/6-31G(d,p)	B3LYP/6-31G(d,p)	Vibrational assignments (PED)
	FTIR	FT-Raman	HF	B3LYP	IR intensity	Raman activity	IR intensity	Raman activity	Force constants		
1		-	52	47	312.69	1.55	257.74	1.32	0.24	0.18	τ NH_2 (61)
2		-	72	85	0.01	0.40	0.01	0.69	0.04	0.04	t CO_2 (54)
3		-	134	135	0.46	3.34	0.44	2.78	0.06	0.06	τ COH (64)
4		173(w)	164	161	1.56	0.78	1.79	0.47	0.10	0.09	γ COH (74)
5		216(w)	203	203	0.68	0.59	0.56	2.02	0.16	0.14	γ C-NH_2 (53) + γ COH (24)
6		280(w)	219	297	0.22	1.32	0.09	1.20	0.04	0.06	t NH_2 (74)
7		-	328	332	8.67	0.64	8.77	0.40	0.42	0.36	γ CN (50)
8		354(w)	364	354	0.25	1.52	0.46	0.70	0.51	0.44	β C-NH_2 (70)
9		-	372	370	2.58	0.97	2.37	1.49	0.45	0.39	β CCC (49) + β COH (29)
10		422(w)	419	410	5.31	3.42	6.25	1.87	1.15	0.32	β CCC (54)
11	464 (w)	-	425	427	11.18	1.43	2.73	5.22	0.39	1.14	γ CO (81)
12	485 (s)	497 (w)	468	464	1.51	9.47	1.57	10.99	1.19	1.03	β CCC (69)
13	539 (vs)	521 (m)	533	527	7.84	0.95	9.63	1.61	0.84	0.73	γ CCC (59)
14	560 (m)	542 (m)	543	531	3.23	1.93	0.00	2.66	0.40	0.41	β CCC (64)
15	570 (w)	588 (w)	585	582	108.13	2.43	105.85	4.90	0.38	0.29	β CCC (77)
16	641 (m)	596 (m)	592	646	138.94	1.32	47.45	1.70	0.27	1.37	γ OH (57)
17	684 (s)	662 (m)	658	675	61.54	0.59	6.05	0.09	1.68	1.21	β OH (43) + β CO_2 (18)
18	687 (w)	704 (w)	703	711	10.51	0.30	72.69	1.28	1.44	0.36	γ CCC (78)
19	714 (w)	742 (w)	724	714	32.75	13.75	14.32	21.37	1.83	1.68	γ CCC (71)
20	772 (vs)	751 (s)	782	753	37.01	10.71	65.48	0.38	2.43	1.65	γ CCC (60)
21	796 (s)	810 (vs)	799	782	70.01	0.20	31.80	11.77	2.62	2.15	γ CCO (74)
22	811 (vs)	857 (s)	849	806	56.16	2.80	22.25	3.64	0.83	0.65	γ CH (68)
23	886 (w)	870 (w)	895	832	9.56	1.72	6.46	2.08	0.89	0.67	γ CH (73)
24	929 (m)	-	913	912	22.59	11.40	0.24	0.95	2.25	0.69	Ring Breathing (85)
25	948 (m)	962 (w)	978	912	0.65	0.33	3.64	13.48	0.92	1.81	γ CH (71)
26	1029 (w)	1036 (s)	1025	1017	51.89	3.67	4.65	2.92	1.27	0.98	ρ NH_2 (66)
27	1087 (w)	1092 (m)	1064	1050	3.99	0.71	45.75	2.55	2.42	2.62	Ring deformation (78)
28	1117 (w)	1100 (w)	1105	1122	272.41	5.73	0.51	4.21	1.84	1.03	ν CC (71)
29	1133 (s)	1158 (m)	1152	1151	200.84	2.93	486.58	19.09	1.79	1.50	β CCH (72)

30	1190 (s)	1194 (s)	1205	1203	142.18	9.97	13.47	0.83	1.65	1.35	γ CCH (73)
31	1242 (m)	1237 (w)	1233	1260	32.42	5.30	137.81	1.68	1.97	2.56	ν CN (56)
32	1266 (m)	1281 (s)	1274	1283	187.51	9.23	38.68	10.40	2.50	3.94	β CH (68)
33	1314 (m)	1312 (s)	1304	1306	8.57	49.32	33.58	29.24	5.90	2.57	ν CH (54)
34	1352 (w)	1361 (s)	1349	1366	55.39	4.75	27.18	23.37	1.91	4.00	ν C-C (36) + ν CO (20)
35	1376 (w)	1389 (w)	1405	1394	278.79	38.57	256.26	34.33	4.38	2.90	ν CO (67)
36	1451 (s)	1448(w)	1455	1437	1.20	4.08	1.26	21.04	5.48	5.00	ν_s CC (81)
37	1493 (s)	1494 (m)	1504	1482	263.34	4.52	260.54	3.54	4.83	4.25	ν_{as} CC (84)
38	1581 (m)	1548 (vs)	1612	1575	66.53	18.78	53.18	12.78	5.52	5.06	ν CC (64)
39	1619 (w)	1608 (s)	1619	1587	93.04	16.31	74.90	9.09	2.79	2.21	δ NH_2 (66)
40	1650 (m)	1666 (w)	1659	1623	93.04	30.69	168.29	35.12	10.34	8.71	ν CO (64)
41	1797 (w)	1769 (w)	1768	1689	493.58	31.84	260.58	51.10	20.17	12.93	ν CO (72)
42	2974 (w)	3021 (m)	3016	3051	19.27	90.53	18.13	103.21	7.17	6.47	ν CH (97)
43	3083 (w)	3059 (w)	3053	3086	9.84	66.43	7.07	31.49	7.37	6.62	ν CH (96)
44	3095 (w)	3088 (m)	3056	3091	3.58	119.12	4.94	162.03	7.37	6.66	ν_{as} CH (99)
45	3384 (w)	3180(m)	3510	3330	69.65	126.95	256.30	79.40	9.31	7.55	ν_s NH_2 (99)
46	3429 (w)	3629 (m)	3630	3514	39.52	49.12	64.20	171.48	10.53	8.23	ν_{as} NH_2 (100)
47	3442 (w)	3690 (m)	3654	3618	248.34	46.04	89.94	153.49	10.28	8.89	ν OH (95)
48	3718 (m)	3737 (w)	3732	3637	162.17	99.88	27.35	58.78	10.72	9.32	ν OH (96)

ν, stretching; ν_s, symmetric stretching; ν_{as}, asymmetric stretching; β, in-plane bending; γ, out of plane bending; δ, scissoring; ω, wagging; ρ, rocking; t, twisting; τ, torsion

The reproductions of observed fundamental wavenumbers are more desirable because they are directly observable in a vibrational spectrum. Comparison between the calculated and the observed vibrational spectra helps us to understand the observed spectral features.

Stretching vibrations

O-H stretching

Special attention is required for OH vibrations of the title molecule. In the OH region, very strong and broad band occur at 3600 – 3400 cm^{-1}[20]. Two OH stretching modes are observed at 3447 cm^{-1} and 3718 cm^{-1} (mode no. 47 and 48) in the FT-IR spectrum for 5A2HBA. One of them is broad while the remaining one has comparatively lower line width. These results suggest that one OH stretching possibly include in the formation of intra molecular hydrogen bonding. Likewise, OH stretching tends to be involved in inter molecular hydrogen bonding, resulting in one broad OH band at 3718cm^{-1}(mode no.48). The OH stretching modes are weakly polarized therefore they are generally not observed in the Raman spectrum. In short, as seen in Fig. 2 (b), multiple OH bands could be attributed to potential inter–intra molecular interactions. However, during the approximate mode explanations, intra–intermolecular interactions should be taken notice as calculations were performed for a single molecule, which disregards intermolecular interactions. For instance, as in the case observed for OH vibrations, OH groups, which possess intra molecular hydrogen bonding, have lower line width and they appear in the high frequency region compared to broad OH vibrational bands indicating intermolecular hydrogen bonding. In the theoretical calculations, the latter was appeared in the high frequency region. The peaks marked with asterisks in Fig. 2 (b) were possibly due to the hydrogen bonding interactions.

C–C ring stretching

The ring carbon-carbon stretching vibrations occur in the region 1625 - 1430 cm^{-1}. In general, the bands are of variable intensity and according to Varsanyi[21], the five bands in this region are observed at 1625-1590, 1590-1575, 1540-1470, 1465-1430 and 1380-1280 cm^{-1}. In the present work, the frequencies observed in the FT-IR spectrum at 1581, 1493 and 1451 cm^{-1} have been assigned to C-C stretching vibrations. The same vibrations appear in the FT Raman spectrum at 1546, 1494 and 1448 cm^{-1}. The theoretically predicted frequencies at 1541, 1495 and 1450 cm^{-1} are in excellent agreement with experimental data by B3LYP/6-31G(d,p) method (mode nos. 38, 37 and 36). The strong laser Raman band for 5A2HBA is observed at 1546 cm^{-1} and medium band at 1087 and 929 cm^{-1} in FT-IR is assigned to the "breathing" mode of the ring. However, the theoretically predicted value does not reveals any such vibration. The in-plane deformation vibration is at higher frequencies than the out-of-plane vibrations.

C–H stretching

Floare et al. [22] assigned the weak to medium intensity bands observed at 3000–3100 cm^{-1} in the IR spectrum and the medium to strong intensity bands in the above region in the Raman spectrum to C-H stretching vibration in the pyridine ring. Also, quantum chemical vibrational study of 3-bromoacetophenone reported by P. Udhayakala et al. [23] identified that the bands at 3238, 3228, 3220 and 3197 cm^{-1} are due to C-H stretching vibrations. With this view, the bands observed at 2974 and 3083 cm^{-1} (mode nos 42 and 43) in the FTIR spectrum and 3021 and 3059 cm^{-1} in the FT-Raman spectrum were assigned to C-H symmetric stretching vibrations. Similarly, the band observed at 3095 cm^{-1} in the FTIR spectrum and 3088 cm^{-1} (mode no 44) in the FT-Raman spectrum was assigned to C-H asymmetric stretching vibration in the pyridine ring C-H modes. The DFT calculation correlates with the experimental assignment better than

the HF method. The bands at 3051, 3086 and 3091 cm^{-1} in DFT values and 3016, 3053 and 3056 cm^{-1} in HF values are due to C-H stretching vibrations.

C–N stretching

Silverstein et al. [24] assigned C–N stretching absorption in the region 1342-1266 cm^{-1}. The spectra of benzene and benzoic acid substituted compounds show the band in the region 1260-1210 cm^{-1}. In analogy with the previous work, the band appears at 1242 cm^{-1} in FTIR spectrum and 1237 cm^{-1} (mode no. 31) in FT Raman spectrum of 5A2HBA are assigned to C–N stretching mode of vibration.

C=O stretching

The band due to C=O stretching vibration is observed in the region 1850-1550 cm^{-1} due to tautomerism, pyrimidines substituted with hydroxyl groups are generally in the keto form and therefore, have a strong band due to carbonyl group[25]. In the present work, the bands observed at 1650 cm^{-1} in FTIR spectrum and 1666 cm^{-1} (mode no. 40) in Raman are assigned to C=O stretching mode of vibrations.

N-H stretching vibrations

Heteroaromatics containing an N-H group show their stretching vibrations in the region [26,27] 3500-3220 cm^{-1}. The position of the absorption in this region depends upon the degree of hydrogen bonding and hence, upon the physical state of the sample or the polarity of the solvent. In the present work, the bands appearing at 3384 cm^{-1} in the FTIR and 3180 cm^{-1} (mode no 45) in Raman spectrum are due to N-H stretching mode.

Bending vibrations

C–C–C bending

The C–C–C bending bands always occur below 600 cm^{-1}. Benzene derivatives [28] have a medium intensity of band in the region 941-404 cm^{-1}. In the present work, the FTIR band observed at 485 cm^{-1} and 539 cm^{-1} (mode nos 12 and 13) are assigned to C–C–C symmetric and asymmetric bending modes of vibration, respectively.

C–C–H bending

The C–H deformation [29,30] frequencies in benzene and its derivatives are found to occur in the region 1200-1050 cm^{-1}. In the present work the bands observed at 1133 cm^{-1} and 1190 cm^{-1} (mode nos. 29 and 30) in FTIR spectrum and the bands at 1158 cm^{-1} 1194 cm^{-1} in FT Raman spectrum of 5A2HBA are assigned to C–C–H symmetric and asymmetric bending, respectively.

NBO analysis

NBO analysis provides a possible 'natural Lewis structure' picture of ø, because all orbital details are mathematically chosen to include the highest possible percentage of the electron density. A useful aspect of the NBO method is that it gives information about interactions in both filled and virtual orbital spaces that could enhance the analysis of intra- and intermolecular interactions. The second order Fock matrix was carried out to evaluate the donor–acceptor interactions in the NBO analysis [31]. The interactions result is a loss of occupancy from the localized NBO of the idealized Lewis structure into an empty non-Lewis orbital. For each donor (i) and acceptor (j), the stabilization energy E(2) associated with the delocalization i→j is estimated as

$$E^{(2)} = \Delta E_{ij} = q_i \frac{F(i,j)^2}{\varepsilon_j - \varepsilon_i}$$

Natural bond orbital analysis provides an efficient method for studying intra and intermolecular bonding and interaction among bonds, and also provides a convenient basis for investigating charge transfer or conjugative interaction in molecular systems. Some electron donor orbital, acceptor orbital and the interacting stabilization energy resulted from the second-order micro-disturbance theory are where qi is the donor orbital occupancy, are εi and εj diagonal elements and F(i, j) is the off diagonal NBO Fock matrix element reported [32,33]. The larger the E(2) value, the more intensive is the interaction between electron donors and electron acceptors, i.e. the more donating tendency from electron donors to electron acceptors and the greater the extent of conjugation of the whole system. Delocalization of electron density between occupied Lewis type (bond or lone pair) NBO orbitals and formally unoccupied (antibond or Rydgberg) non-Lewis NBO orbitals correspond to a stabilizing donor–acceptor interaction. NBO analysis has been performed on the molecule at the DFT/B3LYP/6-31G(d,p) level in order to elucidate the intra molecular, rehybridization and delocalization of electron density within the molecule. The intra molecular interaction are formed by the orbital overlap between bonding (C–C), (C–N), (C–C) and (C–N) anti bonding orbital which results intra molecular charge transfer (ICT) causing stabilization of the system. These interactions are observed as increase in electron density (ED) in C–C, C–N anti bonding orbital that weakens the respective bonds. The electron density of conjugated double as well as single bond of the aromatic ring (∼1.9e) clearly demonstrates strong delocalization inside the molecule.

Table -3 Second order perturbation theory analysis of fock matrix in NBO basis for 5-amino-2-hydroxybenzoic acid (5A2HBA)

Donor (i)	Type	ED/e	Acceptor	Type	ED/e	$^{a}E^{(2)}$ (kj mol^{-1})	^{b}E(j)-E(i) (a.u)	^{c}F(i,j) (a.u)
C_1-C_2	σ	1.96859	C_2-C_3	σ*	0.02674	5.67	1.42	0.08
			C_2-C_7	σ*	0.04204	4.47	1.41	0.071
C_1-O_8	σ	1.99516	C_1-C_2	σ*	0.04997	2.51	1.69	0.059
			C_2-C_3	σ*	0.02674	2.67	1.76	0.061
	π	1.9764	C_2-C_7	π*	0.4685	5.05	0.45	0.048
C_1-O_9	σ	1.99582	C_2-C_7	σ*	0.04204	1.97	1.63	0.051
C_2-C_3	σ	1.96012	C_2-C_7	σ*	0.04204	6.91	1.38	0.087
			C_4-N_{11}	σ*	0.02322	4.48	1.37	0.07
			C_1-C_2	σ*	0.04997	4.31	1.32	0.068
			C_3-C_4	σ*	0.02998	4.36	1.39	0.07
C_2-C_7	σ	1.96052	C_2-C_3	σ*	0.02674	7.15	1.4	0.09
			C_1-C_2	σ*	0.04997	5.27	1.34	0.075
	π	1.6151	C_1-O_8	π*	0.32805	38.86	0.27	0.092
			C_3-C_4	π*	0.40009	20.91	0.32	0.074
			C_5-C_6	π*	0.34304	19.87	0.32	0.071
C_3-C_4	σ	1.95885	C_4-C_5	σ*	0.03139	6.26	1.39	0.083
			C_2-C_3	σ*	0.02674	4.47	1.39	0.071
	π	1.64398	C_2-C_7	π*	0.4685	22.09	0.32	0.077
			C_5-C_6	π*	0.34304	20.57	0.31	0.072
C_3-H_{12}	σ	1.97503	C_4-C_5	σ*	0.03139	5.45	1.17	0.072
			C_2-C_7	σ*	0.04204	5	1.18	0.069
C_4-C_5	σ	1.95934	C_3-C_4	σ*	0.02998	6.22	1.4	0.084
			C_5-C_6	σ*	0.01501	4	1.4	0.067

C_4-N_{11}	σ	1.98771	C_3-C_4	σ*	0.02998	4.15	1.58	0.073
			C_4-C_5	σ*	0.03139	4.03	1.57	0.071
C_5-C_6	σ	1.97056	C_7-O_{10}	σ*	0.02529	4.99	1.13	0.067
			C_4-N_{11}	σ*	0.02322	4.49	1.38	0.07
			C_4-C_5	σ*	0.03139	4.43	1.39	0.07
	π	1.72662	C_3-C_4	π*	0.40009	22.37	0.32	0.078
			C_2-C_7	π*	0.4685	21.25	0.32	0.078
C_5-H_{13}	σ	1.97158	C_3-C_4	σ*	0.02998	5.41	1.19	0.072
			C_6-C_7	σ*	0.02407	4.15	1.19	0.063
C_6-C_7	σ	1.97158	C_2-C_7	σ*	0.04204	5.65	1.4	0.08
			C_5-C_6	σ*	0.01501	4.04	1.4	0.067
C_6-H_{14}	σ	1.97365	C_2-C_7	σ*	0.04204	5.21	1.17	0.07
			C_4-C_5	σ*	0.03139	4.49	1.17	0.065
C_7-O_{10}	σ	1.99241	C_2-C_3	σ*	0.02674	2.49	1.56	0.056
O_9-H_{15}	σ	1.98952	C_1-C_2	σ*	0.04997	4.23	1.38	0.069
O_{10}-H_{16}	σ	1.99154	C_6-C_7	σ*	0.02407	3.69	1.42	0.065
N_{11}-H_{17}	σ	1.98925	C_3-C_4	σ*	0.02998	6.01	1.31	0.08
N_{11}-H_{18}	σ	1.98914	C_4-C_5	σ*	0.03139	6.01	1.31	0.079
O_8	LP(1)	1.95748	C_1-C_2	σ*	0.04997	5	1.27	0.071
			O_{10}-H_{16}	σ*	0.05523	10.29	1.16	0.098
O_8	LP(2)	1.85458	C_1-C_2	σ*	0.04997	10.39	0.91	0.089
			C_1-O_9	σ*	0.08955	32.18	0.68	0.134
			O_{10}-H_{16}	σ*	0.05523	18.86	0.8	0.112
O_9	LP(1)	1.97194	C_1-O_8	σ*	0.025	8.67	1.18	0.09
O_9	LP(2)	1.83162	C_1-O_8	π*	0.32805	46.99	0.34	0.118
O_{10}	LP(1)	1.97368	C_2-C_7	σ*	0.04204	8.39	1.14	0.088
O_{10}	LP(2)	1.8409	C_2-C_7	π*	0.4685	31.5	0.34	0.101
N_{11}	LP(1)	1.79387	C_3-C_4	σ*	0.02998	54.06	0.32	0.123
C_1-O_8	π*	1.9764	C_2-C_7	π*	1.6151	84.79	0.06	0.097

[a] $E^{(2)}$means energy of hyper conjugative interaction (stabilization energy)
[b] Energy difference between donor and acceptor i and j NBO orbitals.
[c] F(i,j) is the Fock matrix element between i and j NBO orbitals.

The strong intramolecular hyperconjugation interaction of the σ and π electrons of C–C to the anti C–C bond in the ring leads to stabilization of some part of the ring as evident from Table 3.

For example the intra molecular hyper conjugative interaction of σ (C_2–C_7) distribute to σ* (C_2–C_3) and (C_1–C_2) leading to stabilization of ~6.0 kJ/mol. This enhanced further conjugate with anti-bonding orbital of π* (C_1–O_8), (C_3–C_4), (C_5–C_6), leads to strong delocalization of 38.86, 20.91 and 19.87 kJ/mol respectively. The same kind of interaction is calculated in the same kind of interaction energy, related to the resonance in the molecule, is electron donating from LP (1) O_8 to the σ* (C_1–C_2) show less stabilization of 5.00 kJ/mol and further LP(2) O_9 conjugate with (C_1–O_8) through antibond, i.e. π* (C_1–C_8) leads to the strong stabilization energy of 46.99 kJ/mol. The π* (C_1–O_8) of the NBO conjugated with π* (C_2–C_7) resulting to an enormous stabilization of 84.79 kJ/mol.

^{13}C and ^{1}H NMR spectral analysis

The isotropic chemical shifts are frequently used as an aid in identification of reactive organic as well as ionic species. It is recognized that accurate predictions of molecular geometries are essential for reliable calculations of magnetic properties. Therefore, full geometry optimization of 5A2HBA was performed at the using HF/6-31G(d,p) and B3LYP/6-31G(d,p) methods.

Then, gauge-including atomic orbital (GIAO) ^{1}H and ^{13}C chemical shift calculations of the compound has been made by same methods. Application of the GIAO [34] approach to molecular systems was significantly improved by an efficient application of the method to the ab initio SCF calculations, using techniques borrowed from analytic derivative methodologies. GIAO procedure is somewhat superior since it exhibits a faster convergence of the calculated properties upon extension of the basis set used. Taking into account the computational cost and the effectiveness of calculation, the GIAO method seems to be preferable from many aspects at the present state of this subject. On the other hand, the density functional methodologies offer an effective alternative to the conventional correlated methods, due to their significantly lower computational cost.

The experimental and calculated values for ^{13}C and ^{1}H NMR are shown in Table 4. As in Fig. 1, the studied molecule shows seven different carbon atoms. Taking into account that the

Table 4 The experimental and predicted ^{13}C and ^{1}H isotropic chemical shifts (with respect to TMS, all values in ppm) for 5A2HBA

Atom	Exp.	HF/6-31G(d,p)	B3LYP/6-31G(d,p)
C1	143.80	161.60	144.13
C2	86.90	94.11	82.67
C3	89.30	101.53	88.98
C4	109.50	121.21	106.35
C5	93.40	104.53	90.60
C6	96.70	107.89	96.78
C7	123.40	130.69	120.44
O8	-	356.61	375.70
O9	-	133.37	162.33
O10	-	60.78	96.07
N11	-	41.77	60.52
H12	8.16	8.12	7.04
H13	6.47	6.66	5.73
H14	6.71	6.78	6.01
H15	6.91	6.96	6.09
H16	3.48	4.24	3.50
H17	4.49	5.28	4.50
H18	4.32	4.96	4.16

range of ^{13}C NMR chemical shift for analogous organic molecules usually is >100ppm [35,36], the accuracy ensures reliable interpretation of spectroscopic parameters. In the present work, ^{13}C NMR chemical shifts in the ring for the title molecule are >100 ppm, as they would be expected (in Table 4). Nitrogen atom shows electronegative property. Therefore, the chemical shift value

of C_4 calculated by HF, B3LYP/6-31G(d,P) levels, which is in the ring were 121.21 and 106.35 ppm, respectively. Experimental C–N (with respect to TMS) is 109.5 ppm. Similarly, six carbon peaks in the ring are observed from 86.90 to 123.40 ppm are calculated from 94.11 to 130.69 ppm for HF and from 82.67 to 120.44ppm for B3LYP levels. Moreover, the pair C_3/C_6 is expected to be isochronous due to signal averaging, and only two signals for the C–H carbons are expected. These results also support our theoretical results as shown in Table 4. Besides, another carbon peak is calculated by HF and B3LYP levels at 161.60 ppm and 144.3 ppm respectively, is observed at 143.80 ppm (C-CO_2).

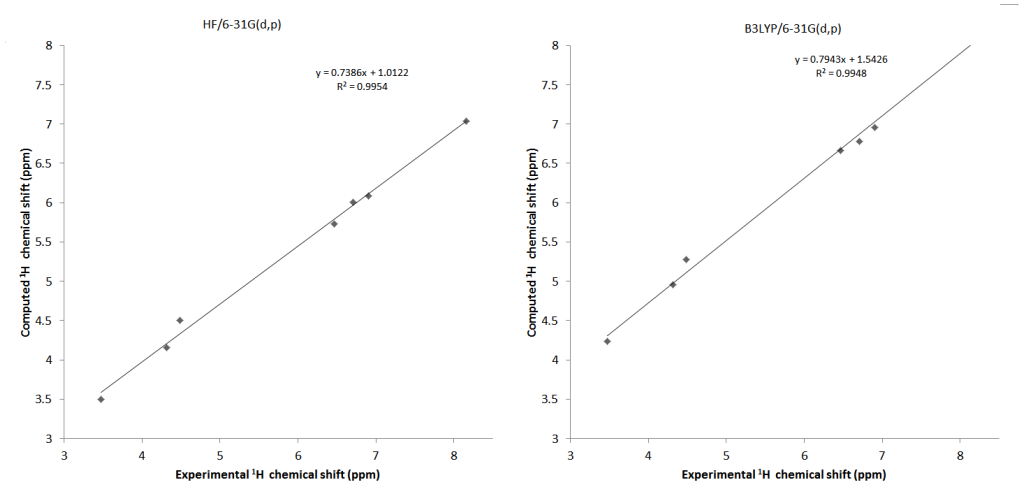

Fig. 7 The relationship between the experimental chemical shift and computed GIAO/HF/6-31G(d,p) and GIAO/B3LYP/6-31G(d,p) levels for ^{1}H

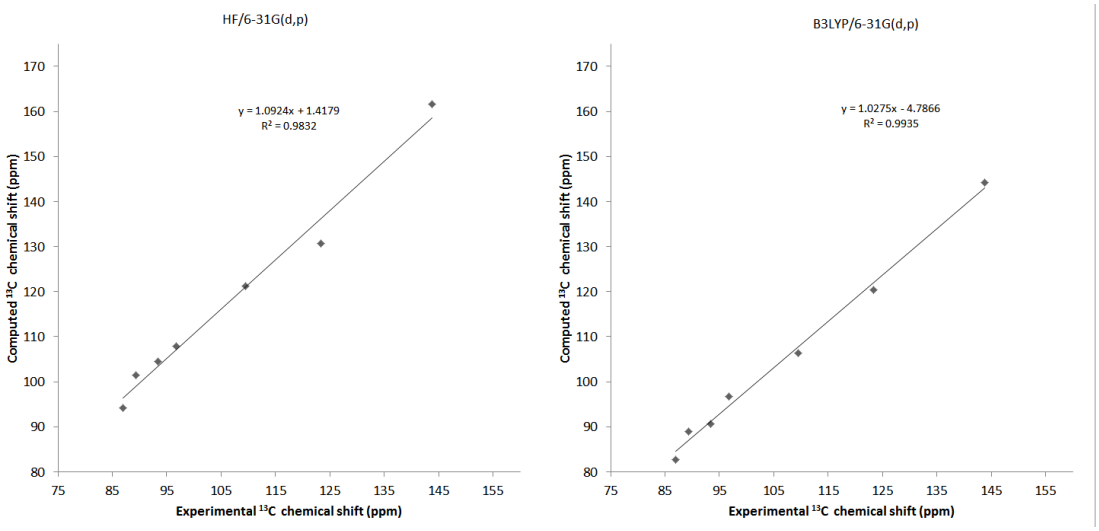

Fig. 8 The relationship between the experimental chemical shift and computed GIAO/HF/6-31G(d,p) and GIAO/B3LYP/6-31G(d,p) levels for ^{13}C

The studied molecule has three hydrogen atoms in the ring, one nitrogen atom attached to the carbon atom of amine group, one oxygen atom attached to carbon atom of hydroxyl group and one carbon atom attached to two oxygen atoms of carboxyl group. In the ^{1}H NMR spectra of NH2, the chemical shift values (with respect to TMS) are 5.28 and 4.96 ppm by HF/6-31G(d,p). In B3LYP/6-31G(d,p) method the values are 4.50 and 4.16 ppm. The remainders of the observed and calculated ^{1}H NMR isotropic chemical shift value are listed in Table 4. As can be seen from Table 4, there is a very good agreement between experimental and theoretical chemical shift results for the title molecule. The relationship between the experimental chemical

shift and computed GIAO/HF/6-31G (d, p) and GIAO/B3LYP/6-31G(d,p) levels for ^{1}H are shown in Fig.7. Similarly, the relationship between experimental chemical shift and computed GIAO/HF/6-31G (d, p) and GIAO/B3LYP/6-31G (d, p) levels for ^{13}C are shown in Fig.8.

HOMO-LUMO Analysis

Many organic molecules, containing conjugated π electrons characterized by large values of molecular first hyperpolarizabilities, were analyzed by means of vibrational spectroscopy [37, 38]. In most of the cases, even in the absence of inversion symmetry, the strongest bands in the Raman spectrum are weak in the spectrum and vice versa. But the intermolecular charge transfer from the donor to acceptor group through a single-double bond conjugated path can include large variations of both the molecular dipole moment and the molecular polarizability, making IR and Raman activity strong at the same time. The experimental spectroscopic behavior described above is well accounted for by *ab initio* calculations in π conjugated systems that predict exceptionally large Raman and infrared intensities for the some normal modes [39]. For 5A2HBA, the corresponding bands in FT-IR and Raman spectra show that the relative intensities in IR and Raman spectra are comparable resulting from the electron cloud movement through π conjugated framework from electron donor to electron acceptor groups. Analysis of the wave function indicates that the electron absorption corresponds to the transition from the ground to the first excited state and is mainly described by one-electron excitation from the highest occupied molecular orbital (HOMO) to the lowest unoccupied molecular orbital (LUMO). The LUMO, of π nature (i.e., benzene ring) is delocalized over the entire C-C and C-N bond. In contrast, the HOMO is located over NH_2 atoms, and consequently the HOMO → LUMO transition implies an electron density transfer to heterocyclic ring from methyl and carbonyl group. Moreover, these orbital significantly overlap in their position for 5A2HBA. The atomic orbital compositions of the frontier molecular orbital are sketched in Fig.9.

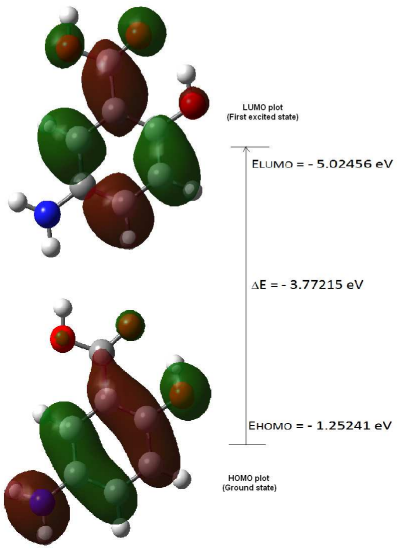

Fig. 9 The atomic orbital HOMO-LUMO composition of the frontier molecular orbitals for 5A2HBA

The HOMO-LUMO energy gap of 5A2HBA calculated at the B3LYP/6-31G(d,p) level reveals that the energy gap reflects the chemical activity of the molecule. LUMO as an electron acceptor represents the ability to obtain an electron, and HOMO represents the ability to donate an electron.

HOMO energy = - 5.02456 eV
LUMO energy = -1.25241 eV
HOMO-LUMO energy gap = - 3.77215 eV

CONCLUSION

In the present study, molecular structure, vibrational frequencies, proton and carbon GIAO NMR shielding of 5-amino-2-hydroxybenzoic acid (5A2HBA) have been studied using HF and DFT calculations. On the basis of the calculated and experimental results; assignment of the fundamental frequencies were examined. Good correlation is found between the computed and experimental wavenumbers. The difference between the observed and scaled wavenumber values of most of the fundamentals is very small. Therefore, the assignments made at DFT level of theory with only reasonable deviations from the experimental values seem to be correct. Therefore, this study confirms that the theoretical calculation of vibrational frequencies for 5A2HBA is quite useful for the vibrational assignments and for predicting new vibrational frequencies. Theoretical 13C and 1H chemical shift values (with respect to TMS) were reported and compared with experimental data, showing a very good agreement both for 13C and 1H. NBO result reflects the charge transfer within the molecule. The theoretically constructed FT-IR and FT-Raman spectra coincide with the experimentally observed spectra. HOMO, LUMO energies and HOMO-LUMO energy gaps has been also discussed.

REFERENCES

[1] E Distrutti; L Sediari; A Mencarelli; B Renga; S Orlandi; G Russo; G Caliendo; V Santagada; G Cirino; JL Wallace; S Fiorucci, *J Pharmacol Exp Ther*., **2006,** 319, 447–458.
[2] S Hussain; J Sharma; M Amir, *E J Chem*., **2008,** 5, 963-968.
[3] S Fiorucci; S Orlandi; A Mencarelli; G Caliendo; V Santagada; E Distrutti; L Santucci; G Cirino; JL Wallace, *Br J Pharmacol*., **2007,** 996-1002.
[4] N Srinivasan; J Lilakar, *Rasayan J Chem*., **2009,** 2, 688-690.
[5] BA Hess; J Schaad; P Carsky; R Zahradnik, *Chem Rev.*, **1986,** 86, 709-730.
[6] P Pulay; X Zhou; G Fogarasi, Recent Experimental and Computational Advances in Molecular Spectroscopy, NATO ASI Series, Vol. C 406 (Ed.: R. Fransto), Kluwer, Dordrecht **1993;** 99-111.
[7] J Andzelm; E Wimmer, *J Chem Phys*., **1992,** 96, 1280-1303.
[8] MJ Frisch; GW Trucks; HB Schlegel et al, Gaussian 03W. Gaussian Inc., Wallingford CT, **2004**.
[9] HB Schlegel, *J Comput Chem*., **1982,** 3, 214-218.
[10] AD Becke, *J Chem Phys*., **1993,** 98, 5648-5652.
[11] GA Zhurko; DA Zhurko, Chemcraft program, Academic version 1.5, **2004.**
[12] JB Foresman; E Frisch, Exploring Chemistry with Electronic Structure Methods. A Guide to Using Gaussian, Gaussian Inc., Pittsburg, PA, **1996.**
[13] JA Pople; AP Scott; MW Wong; L Radom, *Isr J Chem*., **1993,** 33, 345-350.
[14] D Michalska, RAINT Program, Wroclaw University of Technology, Poland, **2003.**
[15] D Michalska; R Wysokinski, *Chem Phys Lett*., **2005,** 403, 211-217.
[16] MH Jamroz, Vibrational Energy Distribution Analysis, VEDA 4, Warsaw, **2004.**
[17] Z Bani Tomisic; B Koji Prodi; I Sirola, *J Mol Struct*., **1997,** 416, 209-220.
[18] G Socrates, Infrared characteristic group frequencies. 1st edn., John Wiley, **1980.**
[19] NB Colthup; LH Daly; SE Wiberly, Introduction to Infrared and Raman Spectroscopy, 2nd edn., Academic Press, New York, **1975.**

[20] Shamoon Ahmad Siddiqui; Anoop Kumar Pandey; Apoorva Dwivedi; Sudha Jain; Neeraj Misra; *J Chem Pharm Res*., **2010**, 2(4), 835-850.
[21] G Varsanyi, Vibrational Spectra of Benzene Derivatives, Academic Press, New York, **1969.**
[22] C Floare; S Astilean; M Bogdan; O Cozar, *Rom J Phys*., **2005,** 50, 815-829.
[23] P Udhayakala; TV Rajendiran; S Seshadri; S Gunasekaran, *J Chem Pharm Res*., **2011**, 3(3), 610-625.
[24] RM Silverstein; G Clayton Basslor; TC Morill, Spectrometric identification of organic compounds, 4th edn., John Wiley, New York, **1981.**
[25] WA Seth Paul, *Spectrochim Acta*., **1974,** 30A, 1817-1833.
[26] S Gunasekaran; R Thilak Kumar; S Ponnusamy, *Spectrochim Acta Part* A., **2006,** 65, 1041-1052.
[27] S Gunasekaran; RK Natarajan; R Rathikha; D Syamala, *Indian J Phys*., **2005,** 79, 509-513.
[28] PM Anbarasan; MK Subramanian; S Manimegalai; K Sugunab; V Ilangovan; N Sundaraganesan, *J Chem Pharm Res*., **2011**, 3(3),123-136.
[29] S Gunasekaran; Leela Abraham, *Indian J Phys*., **2004,** 78B, 485-488.
[30] CJ Pouchert, The Aldrich Library of Infrared Spectra, Aldrich Chemical Co. Inc., Milwakee, Wisconsin, USA, **1975.**
[31] M Szafran; A Komasa; EB Adamska, *J Mol Struct* (THEOCHEM)., **2007,** 827, 101-107.
[32] C James; A AmalRaj; R Reghunathan; I Hubert Joe; VS JayaKumar, J Raman Spectrosc., **2006,** 37, 1381-1392.
[33] LJ Na; CZ Rang; YS Fang, *J Zhejiang Univ Sci*., **2005,** 6B, 584-589.
[34] R Ditchfield, *J Chem Phys.,* **1972,** 56, 5688-5691.
[35] HO Kalinowski; S Berger; S Braun, Carbon-13 NMR spectroscopy, John Wiley and Sons, Chichester, **1988.**
[36] K Pihlaja; E Kleinpeter, Carbon-13 Chemical Shifts in Structural and Stero Chemical Analysis. VCH Publishers, Deerfield Beach, **1994.**
[37] N Sundaraganesan; G Elango; C Meganathan; B Karthikeiyan; M Kurt, *Mol Simulat*., **2009,** 35, 705-713.
[38] T Vijayakumar; I Hubert Joe; CP Reghunadhan Nair; VS Jayakumar, *Chem Phys*., **2008,** 343, 83-99.
[39] MA Palafox, *Int J Quant Chem*, **2000,** 77, 661-684.